

NIGHTJAR: DYNAMIC ADAPTIVE SPECULATIVE DECODING FOR LARGE LANGUAGE MODELS SERVING

Rui Li, Zhaoning Zhang, Libo Zhang, Huaimin Wang, Xiang Fu, Zhiqian Lai

State Key Laboratory of Complex & Critical Software Environment
 National Key Laboratory of Parallel and Distributed Computing
 College of Computer Science and Technology
 National University of Defense Technology
 Changsha, China

ABSTRACT

Speculative decoding (SD) accelerates LLM inference by verifying draft tokens in parallel. However, this method presents a critical trade-off: it improves throughput in low-load, memory-bound systems but degrades performance in high-load, compute-bound environments due to verification overhead. Current SD implementations use a fixed speculative length, failing to adapt to dynamic request rates and creating a significant performance bottleneck in real-world serving scenarios. To overcome this, we propose Nightjar, a novel learning-based algorithm for adaptive speculative inference that adjusts to request load by dynamically selecting the optimal speculative length for different batch sizes and even disabling speculative decoding when it provides no benefit. Experiments show that Nightjar achieves up to 14.8% higher throughput and 20.2% lower latency compared to standard speculative decoding, demonstrating robust efficiency for real-time serving.

Index Terms— Speculative decoding, Large language models serving, Multi-armed bandit, Dynamic real-time request loads

1. INTRODUCTION

Autoregressive (AR) decoding in large language models (LLMs) is often bottlenecked by memory bandwidth, particularly at small batch sizes, leading to underutilized GPU compute [1, 2]. Speculative decoding (SD) [3] mitigates this by using a smaller draft model to generate multiple candidate tokens, which the target model then verifies in parallel. This process is lossless in terms of accuracy and increases concurrency. From a roofline perspective (Fig. 1), SD increases arithmetic intensity by verifying multiple tokens per weight, enhancing GPU utilization in the memory-bound regime typical of low batch sizes. Conversely, as the batch size grows and the system becomes compute-bound, the verification overhead of SD negates its benefits, making standard AR decoding more efficient.

We empirically validate this trade-off¹. As shown in Fig. 2(a), SD provides significant speedups at lower request loads. For instance, a speculative length (γ) of 3 improves throughput by 15.5% at 15 QPS while a speculative length of 2 yielded better improvement than 3 at QPS=25. However, as the load increases, AR decoding surpasses SD's performance. At high loads (Fig. 2(b)), the overhead becomes detrimental, leading to a performance degradation of

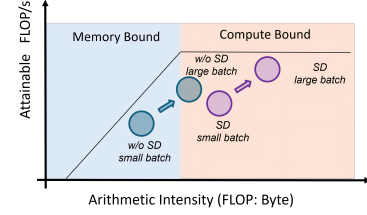


Fig. 1. Schematic roofline illustration of autoregressive decoding (w/o SD) and speculative decoding (SD); positions are illustrative.

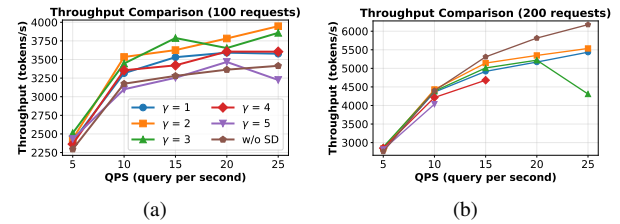


Fig. 2. Throughput under different request loads and rates. γ denotes the speculative length (tokens generated by the draft model per step). Note: Configurations with $\gamma \geq 4$ are omitted at high QPS due to GPU out-of-memory (OOM) errors.

up to 30.25% compared to AR. This confirms that SD excels in the memory-bound regime, while its verification overhead becomes a liability when the system is compute-bound.

The core challenge lies in the dynamic and unpredictable nature of real-world LLM serving loads. Consequently, a fixed speculative length is inherently suboptimal, as a configuration tuned for low-load efficiency can degrade service under high traffic. The optimal speculative length is not a static value but a dynamic variable dependent on real-time factors like system load, hardware characteristics, and token acceptance rates [5].

While various approaches have sought to optimize speculative decoding, they often fail to address the dynamic and unpredictable nature of real-world LLM serving loads. Initial efforts focused on single-request optimization [6, 7, 8, 9, 10] or static offline batches [11, 12], employing predictive algorithms [7] or confidence-based methods [13, 6, 14], but their static nature makes them fundamentally ill-suited for the fluctuating request rates in live environments.

Corresponding author: Zhaoning Zhang, zhangzhaoning@nudt.edu.cn

¹Experiments were conducted on the ShareGPT dataset using vLLM with the DeepSeek-R1-Distill-Qwen-7B model and a 0.5B draft model [4] on an RTX 4090 GPU.

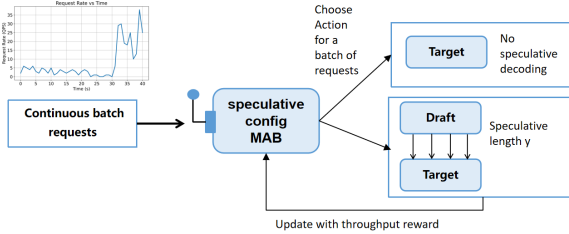


Fig. 3. An overview of our adaptive approach with multi-armed bandit (MAB) for dynamic request load.

More recent works have explored dynamic speculation length adjustment in serving systems [11, 15, 13, 16], yet they exhibit significant limitations. For instance, SpecServe [13] and TETRIS [14] rely on draft confidence scores, but this can lead to poor performance with large batch sizes and still requires generating at least one token. DSD [15] optimizes length via linear goodput modeling, but its reliance on past average acceptance rates introduces a critical vulnerability. This dependency on historical data, found in methods like DSD [15] and SpecServe [13], can lead to a “decision deadlock” where disabling speculative decoding permanently halts the collection of new acceptance rate data, locking the system in a suboptimal state. Our exploration-exploitation approach is designed to mitigate this risk. Even the work of BanditSpec [12], which first introduced a Multi-Armed Bandit (MAB) paradigm, is constrained by its static design, rendering it incompatible with the continuous batching [17] of modern serving systems. Furthermore, to the best of our knowledge, existing works largely overlook the “switching cost” incurred when re-enabling speculative decoding from a length of 0, which is the overhead of KV cache reconstruction for the draft model.

Therefore, the field urgently needs a truly intelligent, adaptive decision-making mechanism that can perceive load changes in real-time and accurately weigh the trade-offs between benefits and costs. It must be capable of dynamically selecting the optimal speculative strategy for different batch sizes at each decoding step—including decisively disabling it when necessary. To address this core challenge, we propose **Nightjar**, a contextual bandit approach for speculative length selection in dynamic, real-time LLM services (Fig. 3). A key feature of our approach is its ability to learn the optimal speculative length for different batch sizes at each decoding step, without requiring prior knowledge of request difficulty or model characteristics. Furthermore, we incorporate the switching cost of transitioning from a speculative length of 0 to a positive value, a factor previously overlooked. Implemented on vLLM [17] and evaluated on three real-world datasets, Nightjar consistently outperforms existing methods, achieving up to 14.8% higher throughput and 20.2% lower latency compared to standard speculative decoding, demonstrating its practical effectiveness for real-time LLM serving.

2. NIGHTJAR ALGORITHM FOR SPECULATIVE LENGTH SELECTION

2.1. Problem Statement

In continual batching [17] for LLM serving, the batch size can vary at each decoding step. We consider batch sizes $B \in \mathcal{B} = \{1, 2, \dots, B_{\max}\}$ and speculative lengths $\gamma \in \{0, 1, \dots, \Gamma_{\max}\}$. Following [15], we evaluate performance using *goodput* $g_{B,\gamma}$, defined as the number of tokens generated per second, including both

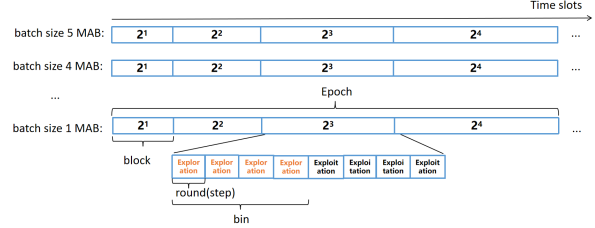


Fig. 4. Illustration of the Nightjar algorithm’s three-level hierarchy. Each batch size maintains its own **Epoch**. Each epoch contains **Blocks** (j_B) of exponentially growing duration, which are responsible for the long-term schedule. These blocks are further divided into fixed-size **Bins** (b_B), the basic units for controlling the exploration-exploitation trade-off. Each **round** (τ_B) is a decoding step.

accepted proposed tokens and bonus tokens generated during verification.

Our objective is to select, for each batch size B , the speculative length γ that maximizes goodput:

$$\gamma^*(B) = \arg \max_{\gamma \in \{0, 1, \dots, \Gamma_{\max}\}} g_{B,\gamma} \quad (1)$$

However, $g_{B,\gamma}$ depends on the token acceptance rate, which is unknown a priori. We model the problem as a regret minimization task over T steps. We define the reward r_{γ}^t as the realized goodput observed after selecting arm γ at step t . The cumulative regret is:

$$R(T) = \sum_{t=1}^T (r_{\gamma_t^*}^t - r_{\gamma_t}^t) \quad (2)$$

Our goal is to find a policy that minimizes $R(T)$.

2.2. Algorithm Design

Contextual MAB can take dynamic request batch size or input sequences as context, such as linear Thompson [18], LinUCB [19], which have been successfully applied in online prediction settings such as configuration selection [20]. However, they are questionable in dynamic serving environments. We adopt the relatively simple framework ADA-BINGREEDY proposed in [21]. One difference between [21] and our approach is that we develop a request batch mechanism to handle varying request patterns. And we design reward that considers the speculative length switch cost.

As shown in Fig. 4, the Nightjar algorithm adaptively selects the speculative length γ for each batch under continuous batching by organizing time into blocks and bins to balance exploration and exploitation.

The decision-making process in Nightjar is driven by an objective function that minimizes the inverse goodput while penalizing frequent re-initializations of the draft model. Formally, at global time t with batch size B , the optimal speculative length γ_t^* for an exploitation step is determined by:

$$\gamma_t^* = \arg \min_{\gamma \in \{0, 1, \dots, \Gamma_{\max}\}} \left\{ \frac{1}{\tilde{g}_{B,\gamma}} + \frac{\mathbb{I}(\gamma_{t-1} = 0 \wedge \gamma_t > 0) \cdot c_{\text{prefill}}}{\gamma_t} \right\} \quad (3)$$

Here, we estimate the empirical mean goodput $\tilde{g}_{B,\gamma}$ using an incremental cumulative moving average to ensure computational efficiency without storing historical reward sequences. Upon observing

a new reward r_t for a specific batch size B and speculative length γ at the n -th visit, the statistic is updated iteratively via $\tilde{g}_{B,\gamma}^{(n)} \leftarrow \tilde{g}_{B,\gamma}^{(n-1)} + \frac{1}{n}(r_t - \tilde{g}_{B,\gamma}^{(n-1)})$, where $\tilde{g}_{B,\gamma}^{(0)} = 0$.

The first term of Eq. (3), $1/\tilde{g}_{B,\gamma}$, is mathematically dual to maximizing the amortized throughput. The second term functions as a regularization mechanism for the switching cost. The indicator function $\mathbb{I}(\cdot)$ activates only when the system transitions from a disabled state ($\gamma_{t-1} = 0$) to an enabled state ($\gamma_t > 0$), incurring a KV cache reconstruction cost c_{prefill} . By dividing this cost by γ_t , the objective favors configurations that amortize the startup overhead across longer speculative sequences, thereby discouraging short-sighted switching that degrades system latency.

Algorithm 1 details the execution flow. To handle the asynchronous nature of continuous batching, Nightjar maintains independent state variables for each batch size B , organizing time into a hierarchical structure of *blocks* (indexed by j_B) and *bins* (indexed by b_B).

Initialization and Bin Selection. For every time step t , the algorithm identifies the current batch size B and determines the strategy for the current bin. As shown in Lines 6–8, at the onset of a new bin (when the round counter $\tau_B = 1$), the bin is designated as an *exploration* bin with probability $1/\sqrt{b_B}$ and as an *exploitation* bin otherwise. This decaying exploration probability ensures that the system explores aggressively in the early stages to gather statistics but progressively converges to the optimal policy as the bin index b_B increases.

Execution and State Evolution. During an exploration bin, the speculative length γ_t is sampled uniformly from the available search space to ensure coverage (Lines 9–11). Conversely, in an exploitation bin, the algorithm selects γ_t by solving Eq. (3) to maximize system efficiency (Lines 12–14). Following the execution of γ_t , the system observes the reward $r_t(\gamma_t)$ and updates the internal counters (Line 15).

A key feature of Nightjar is its exponential time scaling. A bin concludes when the round counter τ_B exceeds $\sqrt{H_B}$, and a block concludes when the bin counter b_B exceeds $\sqrt{H_B}$ (Lines 17–22). Upon the completion of a block, the block size is updated via $H_B \leftarrow 2^{j_B-1}$. This exponential growth ensures that as the history length j_B increases, the duration of stable exploitation phases grows significantly, allowing the system to capitalize on refined goodput estimates.

Prefill Cost Modeling The effectiveness of Eq. (3) relies on an accurate estimation of c_{prefill} , which represents the KV cache reconstruction latency. This cost is not static; it varies based on the hardware state and the synchronization gap between the draft and target models. When speculative decoding is re-enabled, the draft model must process all tokens generated by the target model during the inactive period. We quantify this overhead using the *effective skip length*,

Table 1. Measured switching cost (c_{prefill}) across varying batch sizes and input lengths using a 7B model on an NVIDIA RTX 4090.

Input Length	Batch Size	c_{prefill} (ms)
128	32	17.87
128	64	28.53
256	32	20.65
256	64	22.33
512	32	24.30
512	64	102.03

defined as $L_{\max} = \max\{L_1, \dots, L_B\}$, where L_i is the number of

Algorithm 1: Nightjar Algorithm

```

Input : Max speculative length  $\Gamma_{\max}$ , Max batch size  $B_{\max}$ 
Initialize: Global time  $t \leftarrow 1$ 
1 for  $B = 1$  to  $B_{\max}$  do
2   // Initialize per-batch hierarchy states
3    $j_B \leftarrow 1, H_B \leftarrow 1, b_B \leftarrow 1, \tau_B \leftarrow 1$ 
4 for each time step  $t = 1, 2, \dots$  do
5   Receive current batch size  $B = B_t$ 
6   if  $\tau_B = 1$  then
7     // Bin Initialization
8     Set bin type: Exploration with prob.  $1/\sqrt{b_B}$ , else Exploitation
9   if bin is Exploration then
10    // Uniform Exploration
11    Sample  $\gamma_t \sim \text{Uniform}(\{0, \dots, \Gamma_{\max}\})$ 
12  else
13    // Cost-Aware Exploitation
14    Select  $\gamma_t$  via Eq. (3)
15  Play  $\gamma_t$ , observe reward  $r_t(\gamma_t)$  and update  $\tilde{g}_{B,\gamma}$ 
16   $\tau_B \leftarrow \tau_B + 1$ 
17  if  $\tau_B > \sqrt{H_B}$  then
18    // Bin Completed
19     $b_B \leftarrow b_B + 1, \tau_B \leftarrow 1$ 
20    if  $b_B > \sqrt{H_B}$  then
21      // Block Completed
22       $j_B \leftarrow j_B + 1, H_B \leftarrow 2^{j_B-1}, b_B \leftarrow 1$ 
23   $t \leftarrow t + 1$ 

```

new tokens for request i . Since the draft model verifies the prefix in parallel, the batch latency is determined by the request with the largest lag. The algorithm queries an offline-populated lookup table $c_{\text{prefill}}(L_{\max}, B)$ (Table 1) to obtain the precise cost. For example, empirical profiling on a 13B model indicates that c_{prefill} can range from 5 ms to over 1400 ms depending on L_{\max} , making this dynamic cost retrieval essential for robust decision-making.

Overhead. The arm selection execution time is approximately 1e-5 seconds, while the average generation time per token in the LLM is 0.034 seconds — a difference of nearly 3400 times. This minimal overhead demonstrates the exceptional efficiency of our method, as the cost of dynamic arm selection is negligible compared to the intrinsic latency of token generation.

3. EXPERIMENTS

3.1. Experiment setup

Settings. We select DeepSeek-R1-Distill-Qwen-7B [22] and vicuna-13b [23] as target models and match them with DeepSeek-R1-DRAFT-Qwen2.5-0.5B [4] and vicuna-68m [24] as draft models respectively. The model pair for the 7B target model is operated on a single RTX 4090 (24GB) GPU, and the model pair for the 13B target model operates on an A100 (40GB) GPU. Nightjar is implemented by extending the vLLM (version 0.8.2) [17].

Workloads. We selected real-world production traces from the AzureLLMInferenceDataset [25], and chose a segment with dynamic request rates as shown in Fig. 9. For online chatting, we utilize datasets from ShareGPT [26], Alpaca [27]. For other tasks,

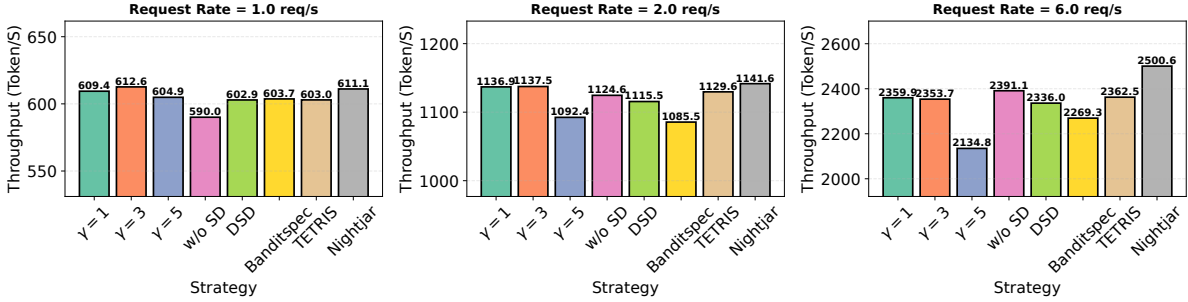


Fig. 5. Method Comparison at Low Request Rate.

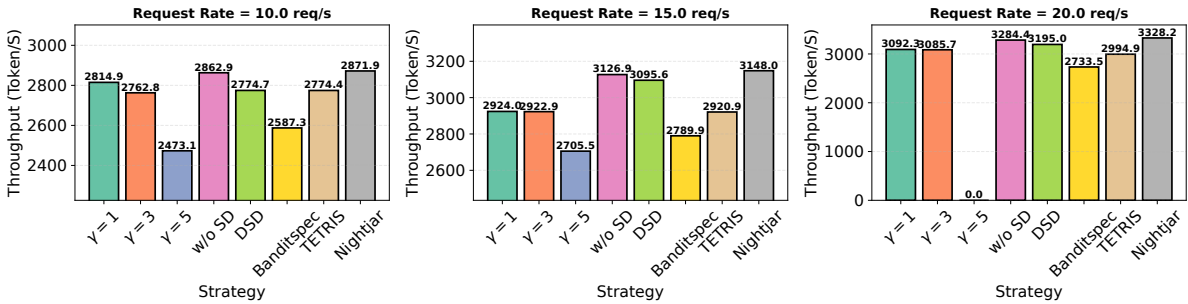


Fig. 6. Method Comparison at High Request Rate.

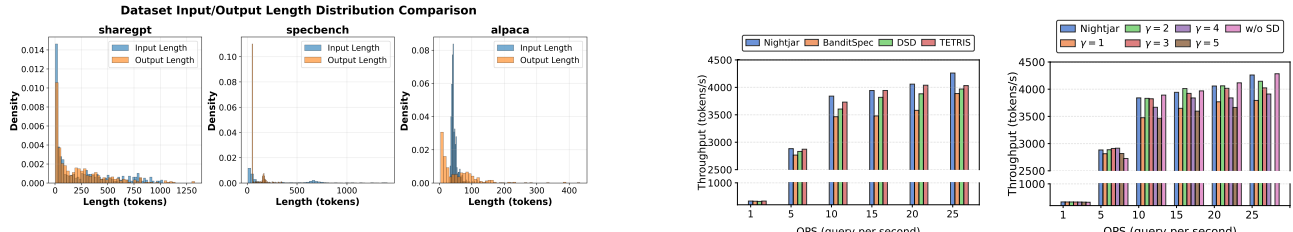


Fig. 7. Distribution of Input and Output Lengths Across Three Datasets.

we utilize SpecBench [1], which is composed of 480 randomly selected instances from six widely used databases. For each dataset, we use 480 instances. The input and output length distribution is presented in Fig. 7.

Baselines. We evaluate the throughput (tokens/s) and mean end-to-end latency of Nightjar against baseline methods: standard speculative decoding (SD, $\gamma = 3$), vanilla decoding without speculative decoding (w/o SD), Dynamic Speculative Decoding (DSD) [15], BanditSpec [12] and TETRIS [14]. Our result is averaged over 5 independent runs.

3.2. Static request load

Nightjar demonstrates robust performance across varying load conditions by dynamically adapting its speculation strategy. In the detailed breakdown by request rate on ShareGPT dataset, under low request rates (Fig. 5) where Speculative Decoding (SD) outperforms standard decoding, Nightjar maximizes efficiency by selecting the optimal draft length. Conversely, in high request rate scenarios

Fig. 8. Throughput comparison for static request rate on SpecBench dataset. (Left) Comparison between SOTA algorithms. (Right) Comparison among different speculative length γ .

(Fig. 6) where the overhead of SD renders it inferior to the baseline, Nightjar adaptively disables speculation to avoid performance degradation, thereby consistently achieving superior results in both regimes. Note that data for $\gamma = 5$ at 20 QPS is excluded from Fig. 6 owing to GPU memory limitations. These advantages are similarly observed on SpecBench dataset (Fig. 8); specifically, Nightjar outperforms baselines at high concurrency (e.g., 25 QPS in Fig. 8(a)) and matches the throughput of the optimal fixed speculative length ($\gamma = 4$) in lower traffic conditions (Fig. 8(b)). This consistent superiority stems from Nightjar’s bandit policy, which dynamically optimizes the speculation length to balance verification costs and generation speed, ensuring optimal efficiency whether the request load is low or high.

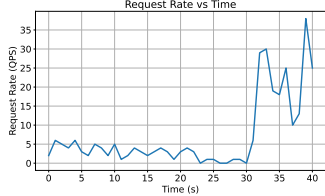


Fig. 9. Request Rate Trace.

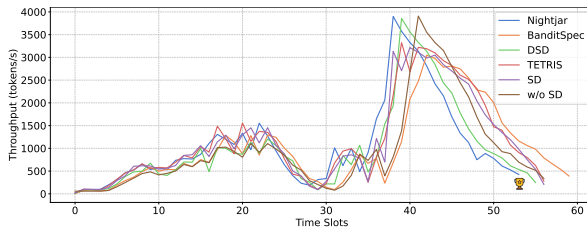


Fig. 10. Throughput Trace.

3.3. Dynamic request load

For 7B model under dynamic request rate (Fig. 9), as shown in Fig. 10, Nightjar surges ahead during low request load periods, achieving the highest peak throughput (3800 tokens/s) and maintaining a consistent lead over rivals during high load phases. DSD’s predictions are less accurate during low request load, leading to throughput degradation, but perform better under high request load, while TETRIS exhibits performance drops under high request load due to its high overhead in large batch size and static BanditSpec is not suitable for dynamic batch size.

Table 2. Throughput (tokens/s) Comparison for 7B and 13B Models

Method	7B			13B		
	Alpaca	ShareGPT	SpecBench	Alpaca	ShareGPT	SpecBench
Nightjar	2102.73	3734.23	3326.20	721.23	1729.68	1061.82
BanditSpec	1860.74	3428.75	2631.43	679.82	1383.81	763.15
DSD	2044.40	3614.65	2789.51	603.32	1244.96	692.01
TETRIS	1875.91	3597.21	2974.14	702.65	1628.86	985.40
SD	1920.63	3593.36	3044.80	628.47	1689.53	964.02
w/o SD	2072.38	3653.61	3207.28	438.13	1290.04	673.48

As shown in Table 2, Nightjar consistently achieves the highest throughput, demonstrating superior scalability over both static and dynamic baselines. While Standard Speculative Decoding (SD) provides moderate gains, Nightjar significantly amplifies these benefits. Notably, on the 13B model, Nightjar achieves a remarkable 64.6% improvement over vanilla decoding (w/o SD) on the Alpaca dataset. More importantly, Nightjar shows exceptional robustness in complex scenarios. Compared to the advanced inference system TETRIS, Nightjar maintains a consistent lead, achieving a 12.1% throughput gain on the 7B Alpaca dataset. Furthermore, on the 13B SpecBench dataset, Nightjar outperforms the competing DSD method by a substantial 53.4% and BanditSpec by 39.1%. Even against the optimized fixed-length SD baseline, Nightjar maintains a clear advantage, proving that its cost-aware policy effectively identifies optimal lengths.

Regarding end-to-end latency, Table 3 further validates Nightjar’s efficiency. For the 7B model, Nightjar reduces latency by 20.2% compared to SD on the Alpaca dataset. Crucially, Nightjar demonstrates superior lightweight scheduling compared to TETRIS. On the

Table 3. Mean End-to-End Latency (ms) Comparison for 7B and 13B Models

Method	7B			13B		
	Alpaca	ShareGPT	SpecBench	Alpaca	ShareGPT	SpecBench
Nightjar	8868.17	6534.76	7618.85	23525.49	8133.92	14691.81
BanditSpec	12340.83	7799.63	9288.23	29077.32	9667.04	19294.42
DSD	9183.21	6499.12	8301.02	16212.44	10057.72	22361.71
TETRIS	11734.19	7409.62	8789.48	22133.43	8046.25	14937.37
SD	11110.68	7047.49	8567.04	24671.40	8152.97	14212.97
w/o SD	8876.14	6438.47	7654.05	32222.49	9350.87	23831.74

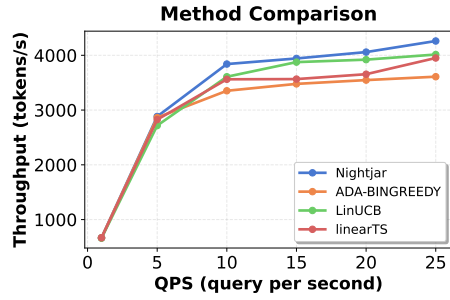


Fig. 11. Performance Comparison of Context-Aware Bandit Methods.

7B Alpaca dataset, Nightjar reduces latency by 24.4% compared to TETRIS, indicating that Nightjar effectively mitigates the complex sampling overheads that hinder TETRIS. On the 13B model, the advantage remains significant against other dynamic baselines: Nightjar reduces latency by 34.3% compared to DSD on SpecBench. This confirms that Nightjar’s bandit-based mechanism avoids the “decision deadlock” and high penalty costs that hamper DSD in high-load, compute-bound environments.

3.4. Ablation Studies

Fig. 11 additionally compares various context-aware multi-armed bandit methods (batch size as context) and the basic ADA-BINGREEDY approach. Our method consistently achieves optimal performance across different QPS levels because LinUCB and linearTS assume linear relationships between rewards and contexts, which don’t hold for LLM speculative serving scenarios. Throughput depends not only on hardware but also on acceptance rates and model types, making linear models unsuitable for this complex scenario.

4. CONCLUSIONS

In this paper, we presented Nightjar, an innovative learning-based algorithm for optimizing speculative decoding. By modeling the speculative length selection as a multi-armed bandit problem, Nightjar dynamically chooses the best decoding strategy for different batch sizes, maximizing throughput and minimizing latency. Extensive evaluations confirm that Nightjar provides superior performance, highlighting a promising direction for more efficient and responsive LLM serving solutions.

5. REFERENCES

- [1] Heming Xia, Zhe Yang, Qingxiu Dong, Peiyi Wang, Yongqi Li, Tao Ge, Tianyu Liu, Wenjie Li, and Zhifang Sui, “Unlocking efficiency in large language model inference: A comprehensive survey of speculative decoding,” in *Findings of the Association for Computational Linguistics: Human Language Technologies 2024*, 2024, pp. 1–16.

citation for Computational Linguistics ACL 2024, Aug. 2024, pp. 7655–7671.

[2] Tianyi Zhang, Yang Sui, Shaochen Zhong, Vipin Chaudhary, Xia Hu, and Anshumali Shrivastava, “70% Size, 100% Accuracy: Lossless LLM Compression for Efficient GPU Inference via Dynamic-Length Float,” Apr. 2025, arXiv:2504.11651 [cs].

[3] Yaniv Leviathan, Matan Kalman, and Yossi Matias, “Fast inference from transformers via speculative decoding,” in *International Conference on Machine Learning*. PMLR, 2023, pp. 19274–19286.

[4] Alamios, “Deepseek-r1-draft-qwen2.5-0.5b,” <https://huggingface.co/alamios/> DeepSeek-R1-DRAFT-Qwen2.5-0.5B, 2024, Accessed: 2025-03-30.

[5] Ranajoy Sadhukhan, Jian Chen, Zhuoming Chen, Vashisth Tiwari, Ruihang Lai, Jinyuan Shi, Ian En-Hsu Yen, Avner May, Tianqi Chen, and Beidi Chen, “Magicdec: Breaking the latency-throughput tradeoff for long context generation with speculative decoding,” *arXiv preprint arXiv:2408.11049*, 2024.

[6] Jikai Wang, Yi Su, Juntao Li, Qingrong Xia, Zi Ye, Xinyu Duan, Zhefeng Wang, and Min Zhang, “Opt-tree: Speculative decoding with adaptive draft tree structure,” *Transactions of the Association for Computational Linguistics*, vol. 13, pp. 188–199, 2025.

[7] Situo Zhang, Hankun Wang, Da Ma, Zichen Zhu, Lu Chen, Kunyao Lan, and Kai Yu, “Adaeagle: Optimizing speculative decoding via explicit modeling of adaptive draft structures,” *arXiv preprint arXiv:2412.18910*, 2024.

[8] Ziyin Zhang, Jiahao Xu, Tian Liang, Xingyu Chen, Zhiwei He, Rui Wang, and Zhaopeng Tu, “Draft model knows when to stop: A self-verification length policy for speculative decoding,” *arXiv preprint arXiv:2411.18462*, 2024.

[9] Oscar Brown, Zhengjie Wang, Andrea Do, Nikhil Mathew, and Cheng Yu, “Dynamic depth decoding: Faster speculative decoding for llms,” *arXiv preprint arXiv:2409.00142*, 2024.

[10] Kaixuan Huang, Xudong Guo, and Mengdi Wang, “Specdec++: Boosting speculative decoding via adaptive candidate lengths,” *arXiv preprint arXiv:2405.19715*, 2024.

[11] Qidong Su, Christina Giannoula, and Gennady Pekhimenko, “The synergy of speculative decoding and batching in serving large language models,” *arXiv preprint arXiv:2310.18813*, 2023.

[12] Yunlong Hou, Fengzhuo Zhang, Cunxiao Du, Xuan Zhang, Jiaochun Pan, Tianyu Pang, Chao Du, Vincent YF Tan, and Zhuoran Yang, “Banditspec: Adaptive speculative decoding via bandit algorithms,” *arXiv preprint arXiv:2505.15141*, 2025.

[13] Kaiyu Huang, Hao Wu, Zhubo Shi, Han Zou, Minchen Yu, and Qingjiang Shi, “Specserve: Efficient and slo-aware large language model serving with adaptive speculative decoding,” *arXiv preprint arXiv:2503.05096*, 2025.

[14] Zhaoxuan Wu, Zijian Zhou, Arun Verma, Alok Prakash, Daniela Rus, and Bryan Kian Hsiang Low, “Tetris: Optimal draft token selection for batch speculative decoding,” *arXiv preprint arXiv:2502.15197*, 2025.

[15] Xiaoxuan Liu, Cade Daniel, Langxiang Hu, Woosuk Kwon, Zhuohan Li, Xiangxi Mo, Alvin Cheung, Zhijie Deng, Ion Stoica, and Hao Zhang, “Optimizing speculative decoding for serving large language models using goodput,” *arXiv preprint arXiv:2406.14066*, 2024.

[16] Zikun Li, Zhuofu Chen, Remi Delacourt, Gabriele Oliaro, Zeyu Wang, Qinghan Chen, Shuhuai Lin, April Yang, Zhihao Zhang, Zhuoming Chen, et al., “Adaserve: Slo-customized llm serving with fine-grained speculative decoding,” *arXiv e-prints*, pp. arXiv–2501, 2025.

[17] Woosuk Kwon, Zhuohan Li, Siyuan Zhuang, Ying Sheng, Lianmin Zheng, Cody Hao Yu, Joseph Gonzalez, Hao Zhang, and Ion Stoica, “Efficient memory management for large language model serving with pagedattention,” in *Proceedings of the 29th symposium on operating systems principles*, 2023, pp. 611–626.

[18] Shipra Agrawal and Navin Goyal, “Thompson sampling for contextual bandits with linear payoffs,” in *International conference on machine learning*. PMLR, 2013, pp. 127–135.

[19] Lihong Li, Wei Chu, John Langford, and Robert E Schapire, “A contextual-bandit approach to personalized news article recommendation,” in *Proceedings of the 19th international conference on World wide web*, 2010, pp. 661–670.

[20] Andreas Stolcke, Anirudh Raju, Colin Vaz, Di He, Venkatesh Ravichandran, Viet Anh Trinh, et al., “Adaptive endpointing with deep contextual multi-armed bandits,” in *ICASSP 2023-2023 IEEE International Conference on Acoustics, Speech and Signal Processing (ICASSP)*. IEEE, 2023, pp. 1–5.

[21] Haipeng Luo, Chen-Yu Wei, Alekh Agarwal, and John Langford, “Efficient contextual bandits in non-stationary worlds,” in *Conference On Learning Theory*. PMLR, 2018, pp. 1739–1776.

[22] DeepSeek, “Deepseek-r1-distill-qwen-7b,” <https://huggingface.co/deepseek-ai/> DeepSeek-R1-Distill-Qwen-7B, 2024, Accessed: 2025-03-20.

[23] lmsys, “vicuna-13b-v1.5,” Hugging Face Model Hub, Accessed: 2025-08-14.

[24] double7, “vicuna-68m,” Hugging Face Model Hub, Accessed: 2025-08-14.

[25] Microsoft Azure, “Azure public dataset,” <https://github.com/Azure/AzurePublicDataset>, 2023, Accessed: 2025-03-20.

[26] anon8231489123, “Sharegpt_v3_unfiltered_cleaned_split_no_imsorry.json,” https://huggingface.co/datasets/anon8231489123/ShareGPT_Vicuna_unfiltered/blob/main/ShareGPT_V3_unfiltered_cleaned_split_no_imsorry.json, 2023, Accessed: 2025-03-20.

[27] Tatsu Lab, “Alpaca dataset,” <https://huggingface.co/datasets/tatsu-lab/alpaca>, 2023, Accessed: 2025-04-15.